Fast scale prototyping for folded millirobots

Aaron M. Hoover
Dept. of Mechanical Engineering
University of California, Berkeley
ahoover@eecs.berkeley.edu

Ronald S. Fearing
Dept. of Electrical Engineering and Computer Science
University of California, Berkeley
ronf@eecs.berkeley.edu

***Abstract*— We present a set of tools and a process, making use of inexpensive and environmentally friendly materials, that enable the rapid realization of fully functional large scale prototypes of folded mobile millirobots. By mimicking the smart composite microstructure (SCM) process at a 2-10X scale using posterboard, and commonly available polymer films, we can realize a prototype design in a matter of minutes compared with days for a complicated SCM design at the small scale. The time savings enable a significantly shorter design cycle by allowing for immediate discovery of design flaws and introduction of design improvements prior to beginning construction at the small scale. In addition, the technology eases the difficulty of visualizing and creating folded 3D structures from 2D parts. We use the example of a fully functional hexapedal crawling robot design to illustrate the process and to verify a scaling law which we propose.**

I. INTRODUCTION

Design and assembly of millimeter-scale robots (millirobots) is time consuming and error prone. A typical millirobot design like the UC Berkeley micromechanical flying insect (MFI) [1] has feature dimensions as small as 125μm, requires unconventional actuators which can be difficult to integrate [11], and is fabricated from composite materials [10] which must be laser micro-machined in a flat configuration, cured, and folded into a functional, articulated structure. Small feature sizes typically necessitate the use of an optical microscope and delicate and careful assembly techniques to ensure kinematic integrity of the completed structure. Integration of unconventional actuators requires the structural design to be exact to enable actuators to deliver the appropriate forces to the structure. And finally, composite materials must be laser micromachined and cured; both of these processes can be time consuming and significantly reduce the rate at which new design improvements can be implemented, typically 3 days minimum from the start of cutting to the finished artifact. For these reasons, the small-scale process is not well suited for use in the early stages of robotic design during which many ideas and designs will explored, but most will be discarded.

In this work we present an exact scaled version of the smart composite microstructure (SCM) process [10] that enables the millirobot designer to produce functional scaled prototypes of a robot design. The process utilizes very low cost, so-called "green" materials and allows for the physical realization of a robot prototype in less than one hour for the basic structure without wiring or actuators at a cost of less than $1 per robot. While the material costs for an SCM robot are similar, the speed of the SCM process is fundamentally limited by composite cure times, laser micromachining times, and difficult hand assembly of very small structures. However, by closely mimicking the SCM process, we enable the designer to produce accurate macro models at anywhere from a 2-10X scale so that kinematic and static loading conditions can be explored quickly with a hands-on model. The speed and negligible material cost of the process significantly shorten the design cycle for an SCM-based millirobot.

To introduce the prototyping tools, we give a brief review of the SCM process used at the small scale to fabricate millirobots. Then, we enumerate the steps necessary to produce scaled prototypes, briefly review design rules adapted from the SCM process for folded, flexure-based robots, and discuss the effects of scaling on the overall performance of a prototype. Finally, as a proof-of-concept for the technology, we demonstrate a functional hexapod robot prototype at a 2X scale using the previously described prototyping process. We also show a version of a true-scale millirobot based on the prototype described.

II. PROCESS OVERVIEW

Because the scaled prototyping process mimicks the SCM manufacturing approach closely, we introduce the prototyping process by way of reviewing the important details of SCM.

A. Review of SCM Process

Robot fabrication at the millimeter scale is inherently difficult with conventional technologies such as continuous revolute joints, bearings, and motors because as component size is reduced, surface forces begin to dominate Newtonian forces [9]. Some MEMS research has been successful in creating robotic mechanisms like hinged joints [8], folded structures [12], and mobile microrobots [3], [5], [2]. However, MEMS processes require an expensive infrastructure and are restricted to a specific set of materials.

SCM was envisioned as an integrated process capable of producing millirobotic mechanisms with μm scale features in a rapid, unified fashion. At the core of SCM is the laser micro-machining of composite fiber laminate to produce rigid components with integrated polymer films for compliant, flexural hinges. The steps of the link and hinge fabrication portion of the SCM process are outlined below and correspond to those illustrated in Fig. 2.

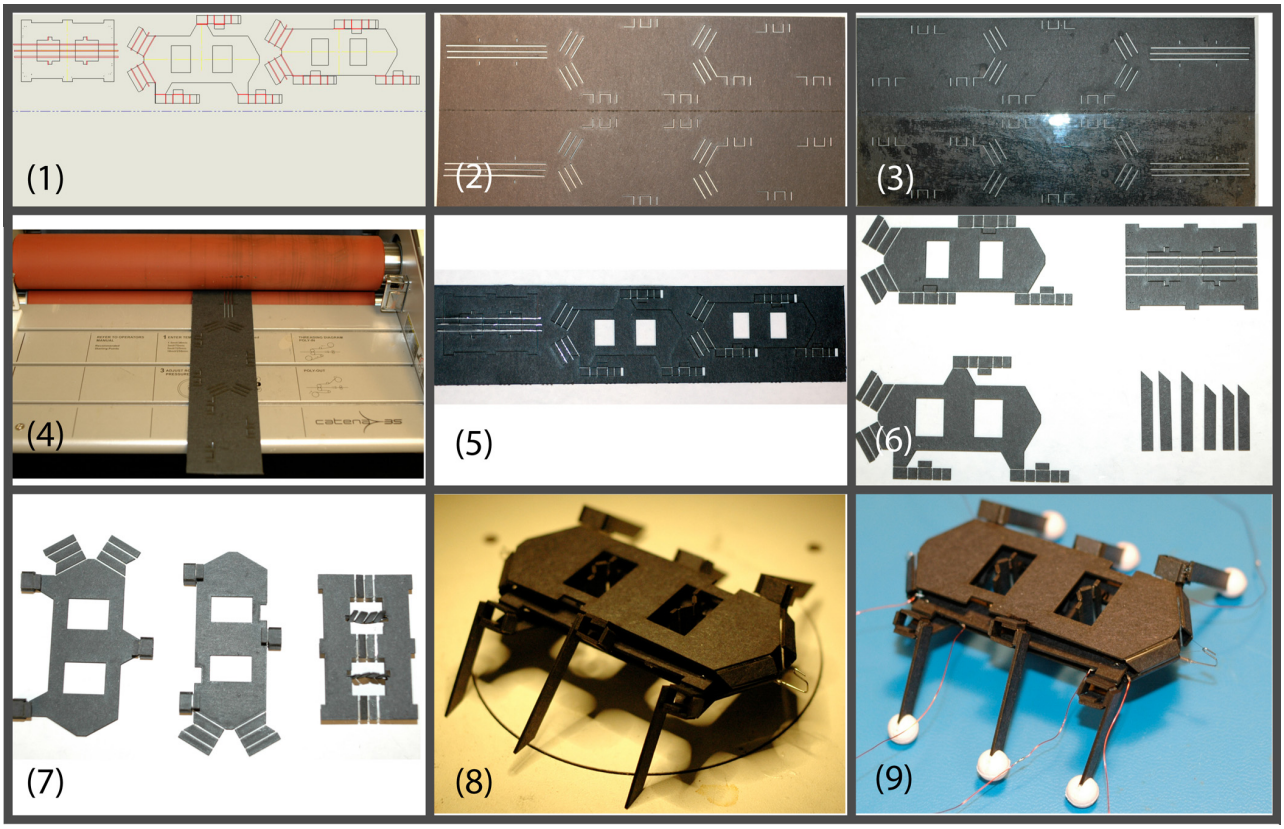

Fig. 1. Steps for prototyping a hexapod crawling robot: **(1)** A 2-dimensional drawing is made in a vector-based illustration program (we use Solidworks). **(2)** A blank piece of posterboard with a pre-cut fold line is folded and placed in a laser cutter, and the flexure cuts are made in both layers. **(3)** The workpiece is removed and adhesive is applied to both sides inside the fold. A 50μm film of PET is sandwiched between the two sides of the fold. **(4)** The workpiece is fed through heated rollers at 230°F at a low speed (approx. 5mm/sec). **(5)** The workpiece is placed back in the laser cutter and outlines of the parts are cut out. **(6)** Parts are released from the workpiece. **(7)** Indiviual linkages can be folded up in place. The three joints on the two leftmost pieces are fourbars used as hips. The joints in the rightmost piece form two Sarrus linkages when two are folded and glued out of plane. **(8)** The three plates are joined such that the hips for one tripod sit above the central plate while the hips for the other sit below, and the legs are attached to the hip fourbars. **(9)** SMA actuators are attached and wired in place and spherical PDMS feet are added.

1) The process begins with a sheet of uncured, pre-impregnated composite fiber laminate.
2) Gaps are laser micro-machined into the composite fiber.
3) A polymer film (typically polyimide) is then placed on top of the laminate.
4) The polymer sheet is cured to the composite fiber.
5) The cured composite and polymer are released and aligned onto another composite fiber layer.
6) The parts are cured.
7) The resulting flat structure is released.

Fig. 3 is an illustration of a flexure hinge created using the SCM process. A layer of polymer film sandwiched between two cured sheets of carbon fiber provide a large range-of-motion compliant flexural joint that is devoid of friction and backlash and as a result does not wear. Entire structures consisting of rigid joints as well as flexible joints can be fabricated in this fashion. The structure can be folded from its flat position into a fully 3D structure - flexure hinges can be glued in place to form permanent rigid joints or left free to serve as compliant hinges for motion transmission as the

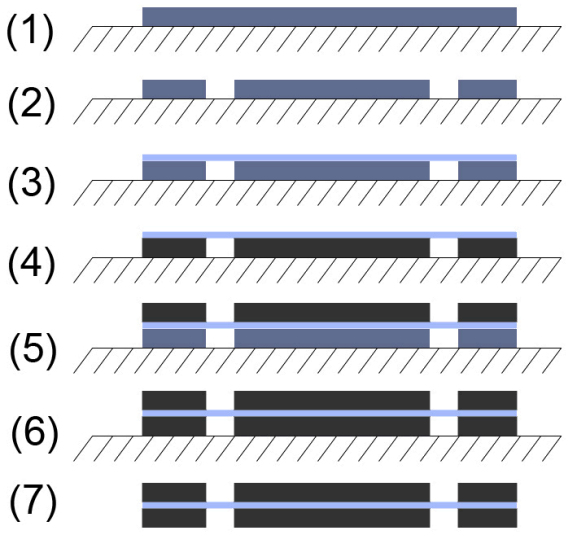

Fig. 2. A step-by-step illustration of the SCM link and hinge fabrication process.

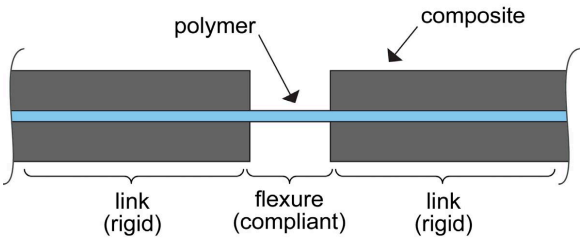

Fig. 3. Schematic illustration of an SCM flexure hinge

design requires. The process has the advantages that an entire articulated robotic structure can be fabricated in a single flat "piece," and, unlike MEMS technology, it can quickly and easily produce truly 3D structures.

B. The Prototyping Process

The macro-scale prototyping process closely follows the SCM process, but instead of pre-impregnated composite fiber laminate, we substitute lightweight, double sided coated posterboard (Nature Saver posterboard, available from Officemax.com). For the polyimide flexure layer, we substitute a thicker polyethylene terephalate (PET) film because thermal compatibility of the film is less of a concern than in the SCM process. In addition, the PET is less inert so it bonds better to various adhesive polymers. Just as in the SCM process, the posterboard is cut using a precision laser (VersaLaser VL200) according to a 2-dimensional design drawing. However, unlike with carbon fiber composites, the posterboard can be easily cut with an infrared laser. The steps for the prototyping process are outlined below with the step numbers corresponding to Fig. 4:

1) The process begins with a sheet of posterboard.
2) Gaps are laser-cut into the posterboard where flexures will be in the final structure.
3) Two layers of adhesive polymer with one layer of flexural polymer (high melting point) are placed between two sheets of posterboard.
4) The resulting structure is rolled through heated rollers to apply pressure and melt the adhesive layers, bonding the structure.
5) Outlines of parts are then laser cut, releasing the parts from the original sheet.

Because the posterboard itself, unlike pre-impregnated composites, contains no adhesive, a simple thermoset polymer film for the flexure layer is insufficient. We must either add adhesive layers separately, or use a polymer film with an integrated adhesive to bond the structure. A carrier film with integrated adhesive is convenient because it's essentially monolithic. However, the standard thicknesses of such films limit the ability of the designer to change the stiffness of flexure hinges by using different thickness films. While it is possible to use more than one layer of such a film, the interaction of the adhesive layers between the carrier film layers creates a noticeable viscoelastic response from

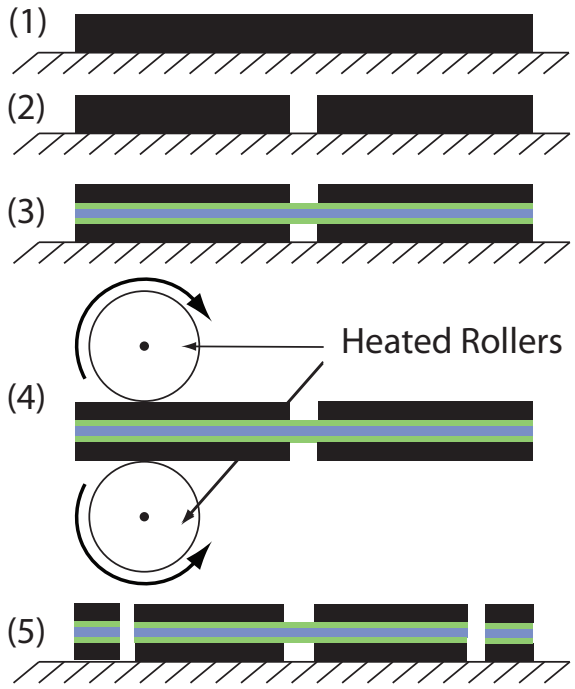

Fig. 4. A step-by-step illustration of the posterboard link and hinge fabrication process

the flexure hinges. In order to retain the flexibility for the designer in the choice of flexure thickness, we have chosen to add a separate adhesive between the posterboard and the flexure film. For the the flexure film we use 50 or 75μm PET depending on the desired flexure stiffness. For the adhesive layer we use UHU ^{TM}glue stick which is a gel-based polyacrylate adhesive.

This prototyping method is appropriate for fabricating entire functional robots or simply mocking up a small mechanism to be integrated into a larger robot design. The hexapod crawler design presented in the following section highlights the difficulty of visualizing a complicated 3D mechanism that results from folding a 2D design. The posterboard prototyping process enables the designer to quickly try out a folded design and explore features such as alignment tabs or self-jamming flexures that can aid significantly in the assembly process. In addition, because the goal of the prototyping process is to produce a large-scale model of a robot that will ultimately be fabricated using anisotropic, directional composites, the prototype can be used to explore folding approaches that ensure that the composite fibers are properly oriented for the loading conditions that will be imposed on the robot. For example, fiber direction should be perpendicular to any movable flexures because the composite laminate is very weak in bending about the fiber axis compared to bending about the axis transverse to fiber direction.

C. Comments on Flexure Design

It is important to address the issue of scaling in order to effectively use the prototypes for predicting mechanism behavior at the small scale. Ideally we would like to develop a scaling law that can be used to prototype at any scale. There are two parameters in which we're interested - the flexure hinge behavior and the stiffness of the structural members or links.

Simple design rules based on modeling flexures using the pseudo-rigid-body model presented in [6] are outlined in [10]. In short, to mostly closely match the behavior of an ideal pin joint, the ratio of the axial stiffness of the flexure to its rotational stiffness should be maximized. This objective is subject to geometric constraints imposed by the maximum elastic strain sustainable in the flexures as well as the maximum angle of rotation of the flexure before the edges of the rigid links on opposite sides make contact and jam given by:

$$\phi_{max} = \frac{l}{t} \tag{1}$$

Eqn. 1 is an important constraint when using the fast scale prototyping process. One limitation of the process is that the posterboard is available only in discrete thicknesses. The material used in our prototypes is approximately 6 times thicker than the true scale material. The implication is that this constraint will be stronger at the larger scale. Thus, we must take care in using the design equations from [10] to design the large scale flexures. However, because we are still designing for linear elastic materials at the large scale (and are even aided by the quasi-static loading conditions) these design equations are still relevant.

It should be noted, however, that unlike design at the small scale, we have given no consideration to dynamic effects resulting from flexure stiffness or link inertias. Because the prototype is intended to be exactly that - simply a prototype - we feel that at this point a dynamic analysis is unecessary. This is not to say, though, that the technology could not be extended to more dynamic structures (in related research we have been able to run prototype structures at 5-10 Hz for thousands of cycles) - that is just not our current aim. In addition, we have not discussed the effects of misalignment because we have observed that our prototype structures show negligible misalignment due to a a folding technique we employ which is shown in more detail in the depiction of the process of building a sample prototype.

D. Developing a Scaling Law

In order to scale the rigid members of a design, we must formulate a way of relating the material properties and geometry of a structure built at the small scale to those of the scaled structure. Because the materials used at the different scales are so different, we propose a dimensionless parameter to relate the actual size structure to the scaled prototype as follows:

$$\xi = \frac{kl_c}{mg} \tag{2}$$

where k is the stiffness of a characteristic link in bending, l_c is a characteristic length, and mg is the weight of the entire structure. This formulation comes from using structural stiffness vs. weight as a performance metric. This dimensionless parameter is also based on the implicit assumption that the robot is operating under quasi-static conditions. For a dynamic scenario, it would be preferable to use a characteristic load rather than the weight of the robot in the denominator. It is our aim to use this ratio as a guide in designing scaled prototypes of folded millirobots. That is, robotic structures at the macro scale will perform similarly to their true scale counterparts in terms of stiffness-to-weight ratio if they have similar values for ξ. In following section, we present one such prototype and compute the value of ξ for the structure and compare it to that of the same structure built from fiber reinforced composites.

III. EXAMPLE PROTOTYPE OF HEXAPOD CRAWLING ROBOT

In this section, we use the example of a hexapod crawling robot to demonstrate the prototyping process and verify our scaling law. We should note that the robot we develop using this prototyping methodology is not simply a toy application. Legged locomotion allows robots to cover fractal terrain efficiently and thus can provide relatively high mobility even at a small scale. By taking advantage of the precision, size, flexibility, and speed that the SCM process enables we aim to produce a 2 g insect-inspired crawling robot for applications from search and rescue to mobile sensor networks.

In the current design, SCM enables us to use redundant parallel kinematics to create a ground-free structure similar to ideas presented in [4] with 60 flexure joints but that weighs only 325mg at true scale. The design is steered simply by adjusting the phase difference and stroke amplitude of the two alternating tripods. Combined with high power density actuators like shape memory alloy wire exciting a resonant mode in the final version, an SCM design could enable high mobility and substantial payload capacity. The exploration and improvement of this design has motivated the development of this prototyping methodology enabling us to quickly resolve problems, introduce improvements, and significantly shorten the design cycle.

The following list enumerates the steps involved in fabricating the robot structure and the numbers correspond with Fig. 1:

1) We begin with a 2D drawing of the robot's constitutive parts in which flexure cuts and outlines are drawn in different colors. This is the drawing that is sent to the laser cutter.
2) A sheet of posterboard (with a pre-cut fold line) is folded and placed in the laser cutter and the flexures are cut out of the folded sheet.
3) The sheet is removed and glue is applied to each side of the folded sheet, and a layer of PET film is placed between the two sides.

4) The sheet is folded and fed through heated rollers to bond the layers.
5) The sheet is placed back in the laser cutter and the outlines of the flat structure are cut out, leaving 3 flat single pieces with integrated flexure hinges.
6) The flat pieces are removed from the rest of the material so that functional linkages can be folded up.
7) Fourbar linkages at the six hip joints are folded up and a plate with a Sarrus linkage used as a translational bearing is folded up as well.
8) The three plates are joined at the fourbar hips and the legs are glued on, producing the final structure.
9) SMA actuators are then attached to the structure and wired, and small polydimethylsiloxane (PDMS) rubber spheres are placed on the ends of the legs to serve as feet. The final robot is also pictured in Fig. 6.

There are three primary pieces in the robot prototype design, and they are pictured in (6) and (7) in Fig. 1. The two similar looking plates are the top and bottom plates of the robot prototype. Each includes the links necessary for folding up three fourbars which altogether form the six hips. Once assembled, each hip is connected to its respective plate (top or bottom) and the middle plate. The hip joint is designed for two degrees of freedom. The first is the rotation of the links of the parallel fourbar. With the leg attached, this is the forward and backward swing of the leg. The other degree of freedom comes from the fact that the hips of the upper (lower) tripod combined with the middle and upper (lower) plate also form a fourbar linkage. When the middle plate contracts, the hips connected to the upper plate cause the legs to pull inward toward the body while the hips connected to the lower plate cause the legs to swing outward away from the body. The upper and lower plate are joined by a Sarrus joint at each of their ends, constraining them to move forward and back together, but allowing them to move up and down with respect to each other. Simplified kinematic models of these two degrees of freedom are shown in Fig. 5. The kinematics are novel in the sense that the robot is fundamentally without a ground.

A. *Verification of Scaling Law*

Based on the prototype design, an initial composite fiber hexapod crawler has also been fabricated at true scale and is pictured in Fig. 6(b). The composite structure and force transmission mechanisms are in place, but the actuators have not yet been fully integrated. However, based on this structure, we can begin to compare the prototype to the true scale version using the scaling law proposed above. The characteristic link we will use to determine the stiffness, k, is the leg link. We also use the leg length as our characteristic length, l_c. To determine the bending stiffness of each leg (posterboard and composite) the leg was clamped at one end and subjected to a known load at the free end. The tip displacement was observed with a video camera and measured on screen at a zoom of approximately 137X. Using these measurements we can compute the value of ξ for both

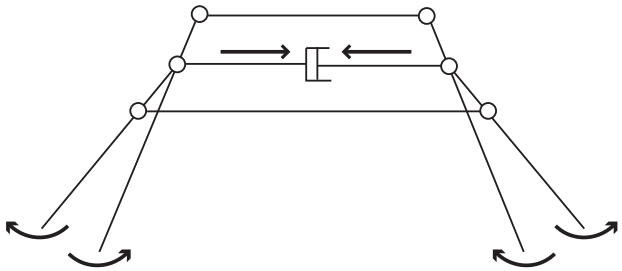

(a) First degree of freedom - into and away from body leg rotation (rear view)

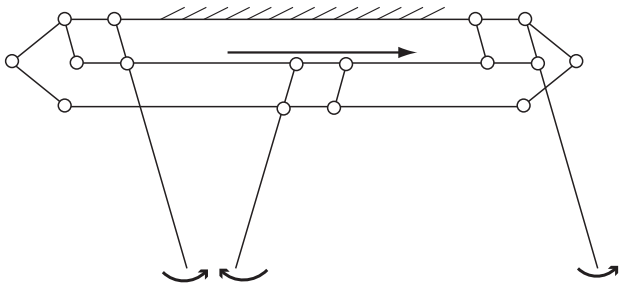

(b) Second degree of freedom - forward and back leg rotation (side view)

Fig. 5. Prototype crawler kinematics showing two independent degrees of freedom

the 2X scale prototype and the composite fiber structure. The measurements and results are summarized in Table I. Overall, the crawler uses 60 flexure joints and 4 structure joints. Unlike conventional robot design, increasing the number of joints has a negligible effect on construction cost or time.

We are encouraged by the fact that the value of ξ for the prototype is within 40% of the value for the composite fiber structure. In fact, the value of ξ for the prototype is higher than for the true scale model. This indicates that the prototype may, in fact, be overpredicting the performance of the composite. This discrepancy can be at least partly explained by the fact that the elastic modulus of paper has been estimated to be on the same order as that for the S-2 glass [7] - approximately 30GPa. In addition, the posterboard is a factor of 3 less dense than the S-2 glass. To even more closely match the prototype to the true scale we could reduce the thickness of the leg links or increase the scaling factor slightly to approximately 2.4X.

B. *Experimental Results*

To demonstrate that the prototype is more than simply a visual tool, ie. it is capable of supporting static loads and enduring cyclical motion, it was wired with three 75μm nickel-titanium shape memory alloy actuators (Flexinol, available from Dynalloy Inc.). While more conventional actuators such as DC motors may provide higher efficiency, better overall power density, and higher bandwidth, SMA was chosen primarily because it enables very easy integration with the folded structure. 2 actuators are run in opposition and drive the forward and back swinging motion of

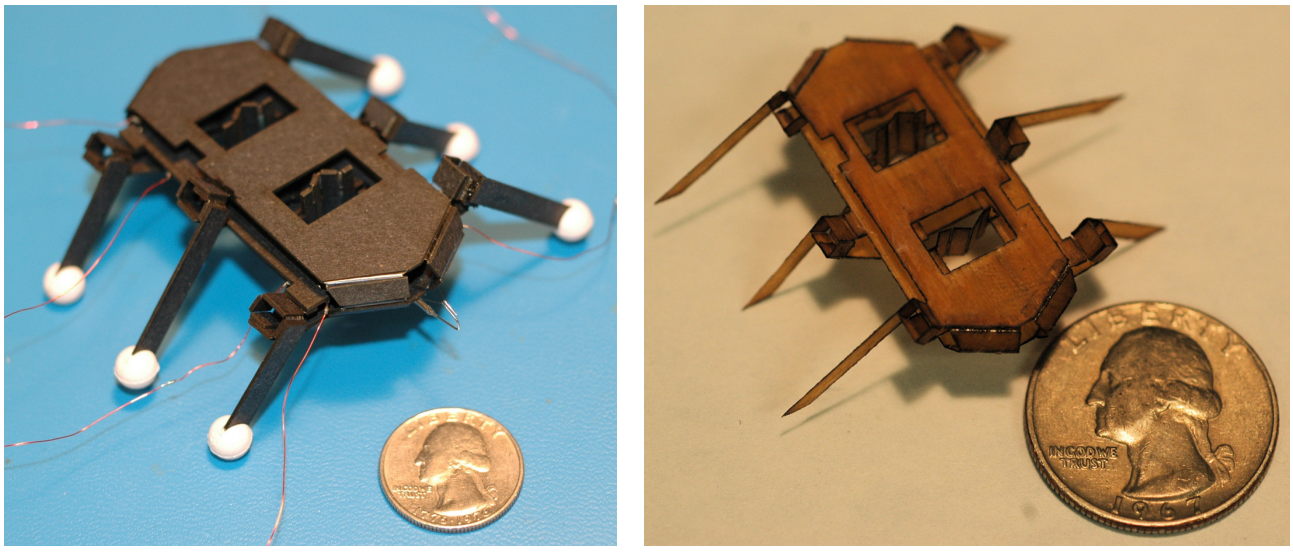

(a) 2X posterboard crawler model

(b) True scale S-2 glass crawler structure

Fig. 6. The scaled prototype structure with actuators integrated and the actual size crawler structure (without actuators or wiring)

TABLE I
COMPARISON OF POSTERBOARD TO S-2 GLASS FIBER COMPOSITE USING EQN. 2

	Posterboard	**S-2 Glass**
l_c	22mm	11mm
b (width)	5mm	2.5mm
h (thickness)	0.875mm	0.15mm
$P_{applied}$	0.01N	0.01N
$\delta_{observed}$	80 x 10^{-6}m	665 x 10^{-6}m
$K_{bending}$	125 $\frac{N}{m}$	66.5 $\frac{N}{m}$
mg	4.6 x 10^{-2}N	3.2 x 10^{-3}N
ρ	750 $\frac{Kg}{m^3}$	2400 $\frac{Kg}{m^3}$
$E_{(11)}$	30 GPa	43 GPa
ξ	84.5	61.1

the legs. One actuator is wired in parallel with a flexural return spring and provides the inward contracting motion that causes the robot to shift its weight from one tripod to the other. The actuators are powered using a constant current circuit which is controlled by digital I/O from a PIC 18f452 microcontroller. Currently, the robot can walk at approximately 1cm/sec (speed is limited strictly by the cooling time required for the SMA actuators) and can be seen climbing a 30° incline in the accompanying video. The crawler has survived over 1000 cycles and is also capable of carrying a payload greater than 4 times its own weight. Fig. 7 shows a series of frames depicting the alternating tripod gait of the robot. The body length is 80mm, width is 50mm, and leg length is 22mm leaving the prototype standing at approximately 15mm without feet. The final mass of the structure of the prototype is 4.7 g without feet and 5.9 g with the addition of spherical PDMS feet.

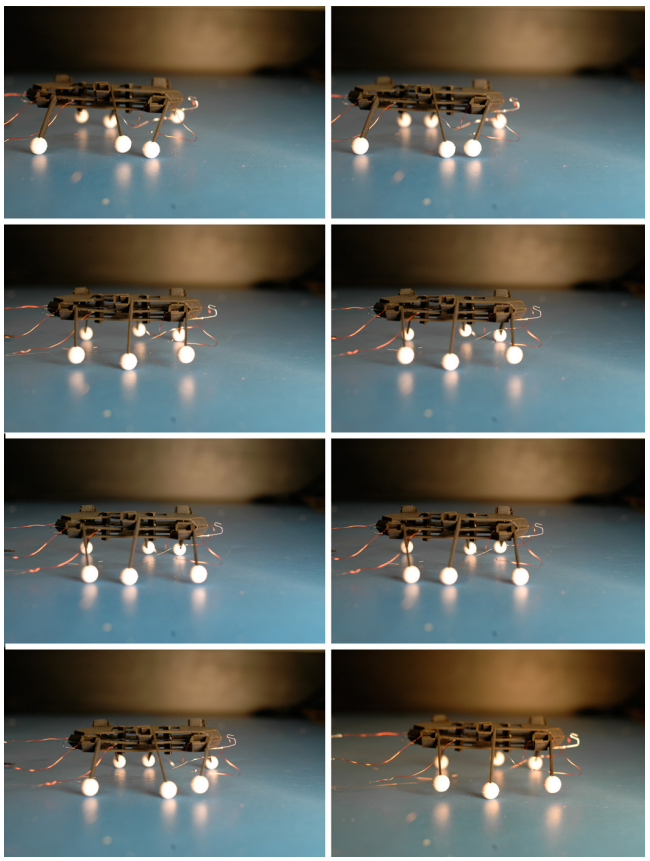

Fig. 7. Time sequence of steps from the robot prototype's alternating tripod gait

IV. DISCUSSION

We have created a scaled version of the SCM process appropriate for rapidly prototyping folded robot designs in a very short period of time. It is our hope that this approach will supplement existing tools and improve the efficiency of design cycle as well as make folded robot design more intuitive with macro-scale models. In addition we have presented a scaling law and shown that it matches our experimental results reasonably well. Lastly, as proof that the prototyping process is complete and capable of producing functional scaled models of millirobots, we demonstrate a sub-5 gram hexapod crawling robot capable of walking at 1 cm/sec.

A. Future Work

The obvious direction for future work is completing the fabrication of the true-scale millirobotic crawling robot and further comparing its performance to the performance of the prototype. In addition, we would like to explore the dynamic behavior of the robot prototypes. Integration with small, lightweight DC motors has begun, but we have not yet reached the point of proposing a dynamic scaling law similar to the one presented here for the quasi-static case.

V. ACKNOWLEDGEMENTS

This work was supported under NSF DMI Grant No. 0423153. The authors thank Erik Steltz for his help, insight, thought-provoking conversations, and patience.

REFERENCES

[1] S. Avadhanula, R. J. Wood, and R. S. Fearing, "Dynamically tuned design of the MFI thorax," in *IEEE Int. Conf. on Robotics and Automation*, Washington, D.C., 2002.

[2] S. Bergbreiter, "Design of an autonomous jumping robot," in *IEEE Int. Conf. on Robotics and Automation*, Rome, Italy, April 2007.

[3] T. Ebefors, J. U. Mattsson, E. Kalvesten, and G. Stemme, "A walking silicon micro-robot," in *10th Intl Conf on Solid-State Sensors and Actuators*. IEEE, 1999, pp. 1202–1205.

[4] M. Goldfarb, M. Gogola, G. Fischer, and E. Garcia, "Development of a piezoelectrically-actuated mesoscale robot quadruped," *J. of Micromechatronics*, vol. 1, no. 3, pp. 205–219, July 2001.

[5] S. Hollar, A. Flynn, C. Bellew, and K. S. J. Pister, "Solar powered 10mg silicon robot," in *IEEE MEMS*, 2003.

[6] L. L. Howell, *Compliant mechanisms*. John Wiley & Sons, 2001.

[7] D. H. Page, "A theory for the elastic modulus of paper," *Brit. J. Appl. Phys.*, vol. 16, pp. 253–258, 1965.

[8] K. S. J. Pister, M. W. Judy, S. R. Burgett, and R. Fearing, "Microfabricated hinges," *Sensors and Actuators*, vol. 33, pp. 249–256, 1992.

[9] W. S. N. Trimmer, "Microrobots and micromechanical systems," *Sensors and Actuators*, vol. 19, pp. 267–287, 1989.

[10] R. J. Wood, S. Avadhanula, R. Sahai, E. Steltz, and R. S. Fearing, "Microrobot design using fiber reinforced composites," *J. Mech. Design*, vol. To appear, 2007.

[11] R. J. Wood, E. Steltz, and R. S. Fearing, "Nonlinear performance limits for high energy piezoelectric bending actuators," in *IEEE Int. Conf. on Robotics and Automation*, Barcelona, Spain, April 2005.

[12] R. Yeh, E. J. J. Kruglick, and K. S. J. Pister, "Surface-micromachined components for articulated microrobots," *J. Microelectromechanical Systems*, vol. 5, pp. 10–17, 1996.